Iranian Journal of Astronomy and Astrophysics
Vol. 10, No. 2, Spring 2023, 221–231
©Available online at http://ijaa.du.ac.ir
DOI: 10.22128/ijaa.2023.731.1167
Online ISSN: 2383–403X

Iranian Journal of Astronomy and Astrophysics

Research Paper

Magnetoacoustic Wave Dynamics and a Magnetic Null-Point

Zeinab Shajei[1] · Zahra Fazel*[2] · Soheil Vasheghani Farahani[3] · Hossein Ebadi[4]

[1] Faculty of Physics, University of Tabriz, Tabriz, Iran;
email: zshaji1107@gmail.com
[2] Faculty of Physics, University of Tabriz, Tabriz, Iran;
*email: z_fazel@tabrizu.ac.ir
[3] Department of Physics, Tafresh University, Tafresh 39518-79611, Iran;
email: s.vasheghanifarahani@tafreshu.ac.ir
[4] Faculty of Physics, University of Tabriz, Tabriz, Iran;
email: hosseinebadi@tabrizu.ac.ir

Received: 12 September 2023; **Accepted:** 28 October 2023; **Published:** 8 November 2023

Abstract. In this study, the interaction of a magnetoacoustic pulse is highlighted with a two dimensional magnetic null point. A simple 2D magnetic null-point in the (x, y) plane is subject to a circlular pulse where its initial starting point depends on solar atmospheric conditions. An analytic relation is presented that governs the density perturbations due to the nearing of the magnetoacoustic pulse. This enables a deeper insight on the effects of the zero and finite plasma-β conditions on the density perturbations. The analytic results are accompanied by numerical plots using the PLUTO code. The results indicate that finite plasma-β conditions decrease the plasma density at the magnetic null-point. Adequate evidence for considering atmospheric conditions to prevent inaccurate conclusions regarding the interaction and energy transfer.

Keywords: Sun, Magnetohydrodynamics, Magnetic null point.

1 Introduction

The solar wind acceleration and coronal heating are two aspects of the solar atmosphere that comprise many physical phenomena. Some features of the solar atmosphere are somehow independent but some seem to be part of a chain reaction. An example of the latter is that the constitution of a magnetic quadrupole established by the presence of two loops experiences a current sheet over the bigger loop which starts to get instable due to the evolving smaller loop creating a reconnection site where outflows are ejected [1,2]. The outflows depending on their sizes are named as type I, II spicules or jets [3,4].

The physics underlying such a series is not well understood without finding out the topology [5–7] and behavior of the magnetic fields, especially the role of the magnetic null point [8–11] which features in the reconnection site. In the context of the present study, the results and conclusions are extracted from the magnetohydrodynamic (MHD) theory [12]. However, various phenomena have been studied analytically and numerically to justify coronal heating [13]. The fact of the matter is that besides studying Alfven waves in solar jets and loops [14,15] focus must also be made on Alfven waves approaching magnetic null

* *Corresponding author*

points which results in the induction of fast and slow magnetoacoustic waves [11,16,17] besides its coupling with compressive waves [8,18] all provides contribution towards coronal heating due to dissipation processes [11,19].

Before proceeding to the theory and model, it is worth stating a brief history regarding magnetic null points in the solar corona. The study of magnetic null points came to prominence when its oscillatory behaviour [7,20] together with its evolution was highlighted [5,6] which were two dimensional studies succeeding the model provided in order to character waves around two-dimensional magnetic null points which indicated that Alfven waves and magnetoacoustic waves act different [22]. This provided basis to state that various modes propagate separately [18,23].

In the context of the present study the aim is to shed further light on the behaviour of an $m = 0$ fast magnetoacoustic pulse observed by McLaughlin & Hood while approaching a 2D magnetic null point [8] for various atmospheric conditions. To state clearer, when the circular $m = 0$ magnetiacoustic pulse experiences a deformation while approaching the null point, it tends to look like an $m = 2$ magnetoacoustic pulse which could be explained by a nonlinear partial differential equation [21]. However, a radial magnetoacoustic pulse nearing a magnetic null-point in coronal conditions has been proved to trigger reconnection due to radial disturbances. The outcome would be a fast-oscillating behaviour which depends logarithmically on the plasma resistivity [24,25]. Nonetheless, McLaughlin considered an initially cylindrically-symmetric fast magnetoacoustics wave in the neighbourhood of a two-dimensional magnetic null point for zero and finite plasma-β values. The fact of the matter is that wave interaction with magnetic null points would shed light on highly energetic solar flares [26].

In the present study, although the main results regarding the compressive perturbations approaching a 2D magnetic null point are obtained numerically, but to provide further insight on the effective parameters that shape the behviour of the physical perturbations in the neighbourhood of a 2D magnetic null-point, analytic equations are also obtained. This is in a sense that an analytical solution for the mass density using a circular primary fast magnetoacoustics pulse at $t = 0$ is provided. Then, the numerical simulations are carried out using the PLUTO code [19] that is a finite-volume, shock-capturing code which its computation is based on a double precision arithmetic [27–29].
In the following section, the basic equations are represented together with the initial setup. In Section 3, the Alfven wave nearing a magnetic null point is simulated. Finally, in Section 4, we provide a brief conclusion and outlook.

2 Model and analytical formulation

In the context of the present study, the analytic and numerical results are based on the MHD theory. The model implemented is a follow up of the work carried out by Gruszecki et al. (2011) and Sabri et al. (2018) by considering finite plasma-β conditions [10,21]. It is

worth stating the well-known resistive MHD equations in the presence of gravity as [11]

$$\frac{\partial \rho}{\partial \mathrm{t}} + \nabla.\left(\rho \mathbf{v}\right) = 0\,, \tag{1}$$

$$\rho\left[\frac{\partial \mathbf{v}}{\partial \mathrm{t}} + \rho\left(\mathbf{v}.\nabla\right)\mathbf{v}\right] = -\nabla \mathrm{P} + \frac{1}{\mu}\left(\nabla \times \mathbf{B}\right) \times \mathbf{B}, \tag{2}$$

$$\rho\left[\frac{\partial \epsilon}{\partial \mathrm{t}} + \left(\mathbf{v}.\nabla\right)\epsilon\right] = -\mathrm{P}\nabla.\mathbf{v} + \frac{1}{\sigma}|\mathbf{J}|^2 + \Lambda, \tag{3}$$

$$\frac{\partial \mathbf{B}}{\partial \mathrm{t}} = \nabla \times \left(\mathbf{v} \times \mathbf{B}\right) + \eta \nabla^2 \mathbf{B}. \tag{4}$$

It is worth noting that the magnetic field $\mathbf{B}$ satisfies the condition $\nabla \cdot \mathbf{B} = 0$ and the relation for the electric current density obeys $\mathbf{J} = \nabla \times \mathbf{B}/\mu$, while the physical variables ρ, p, and $\mathbf{v}$ represent the density, plasma pressure, and velocity, respectively. In addition, $\mu = 4\pi \times 10^{-7} Hm^{-1}$ is the magnetic permeability, σ is the electrical conductivity which is inversely proportional with the magnetic diffusivity η, ϵ represents the internal energy density equal to $P/\left[\rho\left(\gamma - 1\right)\right]$, and Λ represents the volumetric energy gain/loss terms. In the context of the present study, the ratio of the specific heats γ is equal to 5/3, see also Karampelas et al. (2022). The initial magnetic field is given by $\mathbf{B} = \mathbf{B_0}\left[x/L,\, -y/L, 0\right]$, where $\mathbf{B_0}$ is the strength of the magnetic field and L is a characteristic length scale. The velocity profile of the initial magnetoacoustic pulse in the $x - y$ plane is defined as [8,21] (see Figure 1).

$$V_x = \mp A_0 \sin\left(\pi \frac{\sqrt{x^2 + y^2} - r_1}{r_0}\right) \frac{{B_y}^2}{{B_x}^2 + {B_y}^2}, \tag{5}$$

$$V_y = \mp A_0 \sin\left(\pi \frac{\sqrt{x^2 + y^2} - r_1}{r_0}\right) \frac{{B_x}^2}{{B_x}^2 + {B_y}^2}. \tag{6}$$

We consider the circular initial fast magnetoacoustics pulse with the center at the origin where its circumference is equal to $2\pi r_1$

$$r_1 < \sqrt{x^2 + y^2} < r_1 + r_0. \tag{7}$$

To provide a better description regarding the probable cases, two situations regarding the signs are illustrated:
1- Both signs are negative or both are positive

$$V_x = A_0 \sin\left(\pi \frac{\sqrt{x^2 + y^2} - r_1}{r_0}\right) \frac{{B_y}^2}{{B_x}^2 + {B_y}^2}, \tag{8}$$

$$V_y = A_0 \sin\left(\pi \frac{\sqrt{x^2 + y^2} - r_1}{r_0}\right) \frac{{B_x}^2}{{B_x}^2 + {B_y}^2}. \tag{9}$$

In order to provide an analytical solution for the density perturbations, we write V_x and V_y in polar coordinates. Thus, we have

$$\begin{bmatrix} V_r \\ V_\theta \end{bmatrix} = \begin{bmatrix} cos\theta & cos\left(90 - \theta\right) \\ \cos\left(90 + \theta\right) & cos\theta \end{bmatrix} \begin{bmatrix} V_x \\ V_y \end{bmatrix}, \tag{10}$$

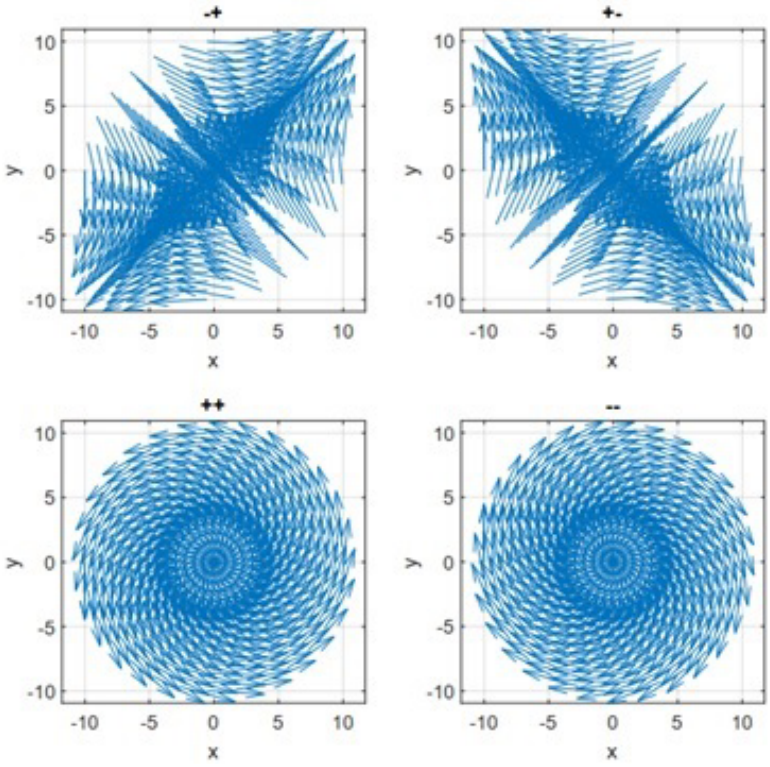

Figure 1: Vector field of circular initial fast magnetoacoustics pulse.

where

$$V_r = cos\theta\ V_x + sin\theta\ V_y, \tag{11}$$

$$V_\theta = -sin\theta\ V_x + cos\theta\ V_y. \tag{12}$$

By inserting V_x and V_y in equation (11) and equation (12), we have

$$V_r = 0, \tag{13}$$

$$V_\theta = \frac{A_0 L}{B_0} \sin\left[\frac{\pi}{r_0}(r - r_1)\right] \frac{1}{r}, \tag{14}$$

Using equation (1) one can obtain

$$\frac{\partial \rho_1}{\partial t} = -V.\nabla\rho = -V_r \frac{\partial \rho_1}{\partial r} - \frac{1}{r} V_\theta \frac{\partial \rho_1}{\partial \theta} \tag{15}$$

Substitute V_r and V_θ in equation (15) one can get

$$\frac{\partial \rho_1}{\partial t} = -\frac{A_0 L}{B_0} \times \frac{1}{r^2} \sin\left[\frac{\pi}{r_0}(r - r_1)\right] \frac{\partial \rho_1}{\partial \theta}. \tag{16}$$

Now, we calculate ρ by the method of separation of variables. We look for solutions that are simple products,

$$\rho_1 = u(r, \theta)\, \varphi(t), \tag{17}$$

where $u(r, \theta)$ is a function of r and θ while $\varphi(t)$ is an only a function of time.

Apparently, this is an absurd restriction, and we cannot hope to obtain more than a tiny subset of all solutions in this way. Nonetheless, the solutions provide great interest. Moreover, as is typically the case with separation of variables, we are able to finally patch together the separable solutions in such a way as to construct the most general solution.

$$\frac{\partial \rho_1}{\partial t} = -\frac{A_0 L}{B_0} \times \frac{1}{r^2} \sin\left[\frac{\pi}{r_0}(r - r_1)\right] \frac{\partial \rho}{\partial \theta} = -a \frac{\partial \rho}{\partial \theta}, \tag{18}$$

where

$$a = \frac{A_0 L}{B_0} \times \frac{1}{r^2} \sin\left[\frac{\pi}{r_0}(r - r_1)\right]. \tag{19}$$

For separable solutions, we have

$$u(r, \theta) \frac{\partial \varphi(t)}{\partial t} = -a\varphi(t) \frac{\partial U(r, \theta)}{\partial \theta}. \tag{20}$$

We can rewrite equation (20) as

$$\frac{1}{\varphi(t)} \frac{\partial \varphi(t)}{\partial t} = -\frac{a}{u(r, \theta)} \frac{\partial u(r, \theta)}{\partial \theta}. \tag{21}$$

It could be readily noticed that the left hand side is only a function of t, while the right hand side is a function of r, θ. The only way this can possibly be true is if both sides are in fact constant—otherwise, by varying t, we could change the left side without touching the right side, and the two would no longer be equal. Interestingly, this statement is a subtle but crucial argument. We shall call the separation constant E. Then

$$\frac{1}{\varphi(t)} \frac{\partial \varphi(t)}{\partial t} = E, \tag{22}$$

or

$$\frac{d\varphi(t)}{\varphi(t)} = E\, dt. \tag{23}$$

So, one can obtain $\varphi(t) = c_1 e^{Et}$, but we might as well absorb the constant c_1 into u (since the quantity of interest is the product $u\varphi$). Then $\varphi(t) = e^{Et}$. Now, we consider the

$$-\frac{a}{u(r,\theta)}\frac{\partial u(r,\theta)}{\partial \theta} = E, \tag{24}$$

or

$$\frac{du(r,\theta)}{u(r,\theta)} = -\frac{E}{a}\, d\theta. \tag{25}$$

The solution is

$$u(r,\theta) = ce^{-\frac{E}{a}\theta}, \tag{26}$$

where c is a constant. Thus, separable solutions for density is given by

$$\rho_1 = u(r,\theta)\,\varphi(t) = ce^{\left(Et - \frac{E}{a}\theta\right)}. \tag{27}$$

Now, when θ advances by 2π, we return to the same point in space, so it is natural to require that $e^{(-\frac{E}{a}\theta)} = e^{-\frac{E}{a}(\theta+2\pi)}$ i.e $e^{-\frac{E}{a}2\pi} = 1$. From this it follows that $\frac{E}{a} = im$ where m is an integer

$$m = 0,\ \pm 1,\ \pm 2,\ \ldots \tag{28}$$

Hence, the density mass is given by

$$\rho_1 = ce^{(imat - im\theta)} = ce^{im(at-\theta)}. \tag{29}$$

Since, the density must be real we have

$$\rho_1 = c\cos m(at - \theta), \tag{30}$$

on the other hand, $\rho_1(r,\theta,t=0) = \rho_0$. Finally, the analytical solution for the mass density is given by

$$\rho_1 = \rho_0 \cos m(at - \theta), \tag{31}$$

where

$$a = \frac{A_0 L}{B_0} \times \frac{1}{r^2} \sin\left[\frac{\pi}{r_0}(r - r_1)\right]. \tag{32}$$

2- One of the signs is negative and the other is positive Let

$$V_x = -A_0 \sin\left[\frac{\pi}{r_0}\left(\sqrt{x^2+y^2} - r_1\right)\right] \frac{B_y}{{B_x}^2 + {B_y}^2}, \tag{33}$$

$$V_y = A_0 \sin\left[\frac{\pi}{r_0}\left(\sqrt{x^2+y^2} - r_1\right)\right] \frac{B_x}{{B_x}^2 + {B_y}^2}. \tag{34}$$

By inserting the components of the magnetic field, we have

$$V_x = -\frac{A_0 L}{B_0} \sin\left[\frac{\pi}{r_0}\left(\sqrt{x^2+y^2} - r_1\right)\right] \frac{y}{x^2+y^2}, \tag{35}$$

$$V_y = -\frac{A_0 L}{B_0} \sin\left[\frac{\pi}{r_0}\left(\sqrt{x^2+y^2} - r_1\right)\right] \frac{x}{x^2+y^2}. \tag{36}$$

Considering $x = rcos\theta$ and $y = rsin\theta$, we have

$$\begin{aligned} V_r &= cos\theta\ V_x + sin\theta\ V_y \\ &= -\frac{A_0 L}{B_0}\sin\left[\frac{\pi}{r_0}(r-r_1)\right]\frac{rsin\theta}{r^2}cos\theta - \frac{A_0 L}{B_0}\sin\left[\frac{\pi}{r_0}(r-r_1)\right]\frac{rcos\theta}{r^2}sin\theta \\ &= -\frac{A_0 L}{B_0}\sin\left[\frac{\pi}{r_0}(r-r_1)\right]\times\frac{1}{r}sin2\theta, \end{aligned} \tag{37}$$

and

$$\begin{aligned} V_\theta &= -sin\theta\ V_x + cos\theta\ V_y \\ &= \frac{A_0 L}{B_0}\sin\left[\frac{\pi}{r_0}(r-r_1)\right]\frac{rsin\theta}{r^2}sin\theta - \frac{A_0 L}{B_0}\sin\left[\frac{\pi}{r_0}(r-r_1)\right]\frac{rcos\theta}{r^2}cos\theta \\ &= \frac{A_0 L}{B_0}\sin\left[\frac{\pi}{r_0}(r-r_1)\right]\times\frac{1}{r}cos2\theta. \end{aligned} \tag{38}$$

Finally, according to the continuity equation we have

$$\frac{\partial\rho}{\partial t} = -V.\nabla\rho = -V_r\frac{\partial\rho}{\partial r} - \frac{1}{r}V_\theta\frac{\partial\rho}{\partial\theta}. \tag{39}$$

That is

$$\frac{\partial\rho}{\partial t} = \left\{\frac{A_0 L}{B_0}\sin(\frac{\pi}{r_0}(r-r_1))\times\frac{1}{r}\right\}\left[sin2\theta\frac{\partial\rho}{\partial r} + cos2\theta\frac{1}{r}\frac{\partial\rho}{\partial\theta}\right]. \tag{40}$$

It can be seen that for this condition, even for the initial pulse, it is non-trivial to calculate the analytical solution. Therefore, the analytical solution can be obtained only in the special case for the initial pulse at $t = 0$ and in general, it is non-trivial to provide an analytical solution. As time progresses, the initial pulse changes and it becomes difficult to calculate the analytical solution, so in the rest of this paper, using the PLUTO code, we investigate the behavior of magnetoacoustics waves in the neighborhood of a 2.5D null point.

3 Numerical Setup

The setup of the present study is a follow up of the work carried out by Karampelas et al. (2022) [29] with concentration on the plasma density spikes due to variations of the atmospheric conditions especially the plasma-β. The PLUTO code which is an appropriate tool for working with models based on the MHD theory. PLUTO is a finite volume shock capturing code [23]. Various aspects of the numerical procedure in cartesian coordinates are as follows; the time step is calculated due to the third order Runge-Kutta method. The spatial integration is carried out with the fifth order monotonicity preserving scheme (MP5) together with the total variation diminishing Lax-Friedrich solver (TVDLF). It is worth noting that the code variable represented by U_c is obtained by normalizing the unit U by U_0 appropriate for the various solar atmospheric and plasma-β conditions. Here, we considered the simulation in a domain with $(-10, 10) \times (-10, 10)$ Mm and 15001500 grid points. In the following the typical values of the initial pulse and conditions are set as $L_0 = 10^6 m$ is the unit length, $\rho_0 = 10^{-12} Kg/m^3$ the unit density, $B_0 = 10^{-3}(T)$ the unit magnetic field, $v_0 = 0.129\frac{Mm}{s}$ the unit velocity, $r_1 = 5Mm$, $r_0 = 1Mm$ and $A_0 = 10^3 m/s$, see [10,21].

Figure 2 displays the radial velocity of the magnetoacoustic pulse nearing the magnetic null point for two atmospheric conditions represented by $\beta = 0$ and $\beta = 1$ for three snapshots

observed at time instances $t = 0s$, $t = 1s$ and $t = 1.7s$. As can be seen from this Figure 2, the changes of the radial velocity of the pulse depends on the plasma β. To provide further insight, the absolute values of the radial velocity along the line $y = x$ are shown in Figure 4. In order to provide a conclusive result, the variations of the mass density due to the plasma- β conditions also need to be observed. This, dependency of the mass density on the plasma-β is illustrated in the three snapshots of Figure 3. Figure 3 shows that the density variations are completely dependent on the plasma β, which is clearly shown in the Figure 5 along the line $y = x$.

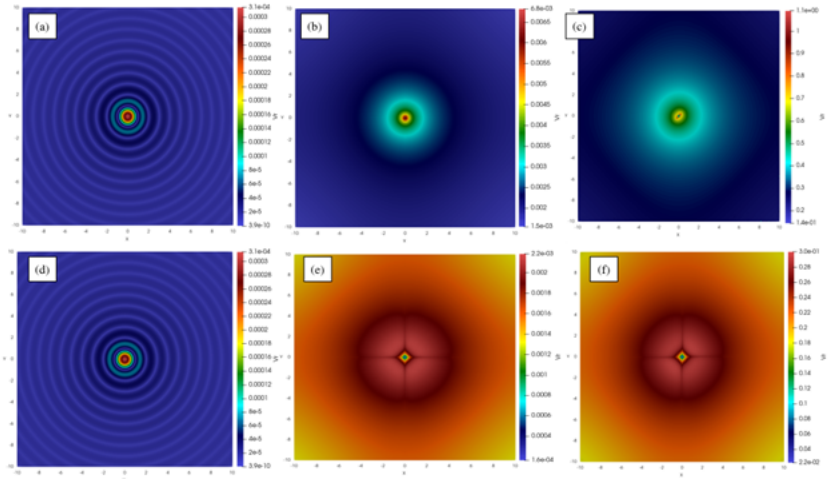

Figure 2: Snapshots of the radial velocity in the inwardly propagating pulse of rarefaction, $v_r = \sqrt{v_x^2 + v_y^2}$ as a function of the radial coordinate r for a) $\beta = 0$ and $t = 0$, b) $\beta = 0$ and $t = 1$, c) $\beta = 0$ and $t = 1.7$, d) $\beta = 1$ and $t = 0$, e) $\beta = 1$ and $t = 1$, f) $\beta = 1$ and $t = 1.7$.

4 Discussion

In this study, we showed that the interaction of fast magnetacoustic waves with a magnetic null-point is dependent on atmospheric conditions where in the context of the present study is represented by the plasma-β. The analytical solution obtained regarding the mass density perturbations is confirmed by the numerical results which clearly show that the wave amplitude decreases for finite plasma-β conditions in comparison with zero plasma-β conditions while nearing the null point. The finite plasma-β conditions also affects the radial velocity causing it to reduce in comparison to zero plasma-β conditions. These results demonstrate the importance of considering the plasma-β and the initial pulse location when studying the interaction of magnetoacoustics waves with magnetic null points.

Acknowledgment

The authors gratefully acknowledge several discussions with Giancarlo Mattia and Konstantinos Karampelas Chiel for their valuable instructions regarding the PLUTO code.

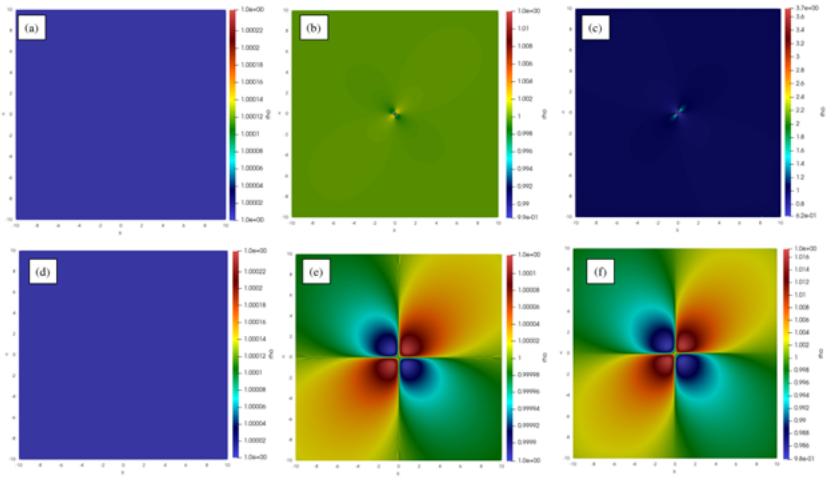

Figure 3: Snapshots of the plasma density in the inwardly propagating pulse of rarefaction, for for a) $\beta = 0$ and $t = 0$, b) $\beta = 0$ and $t = 1$, c) $\beta = 0$ and $t = 1.7$, d) $\beta = 1$ and $t = 0$, e) $\beta = 1$ and $t = 1$, f) $\beta = 1$ and $t = 1.7$.

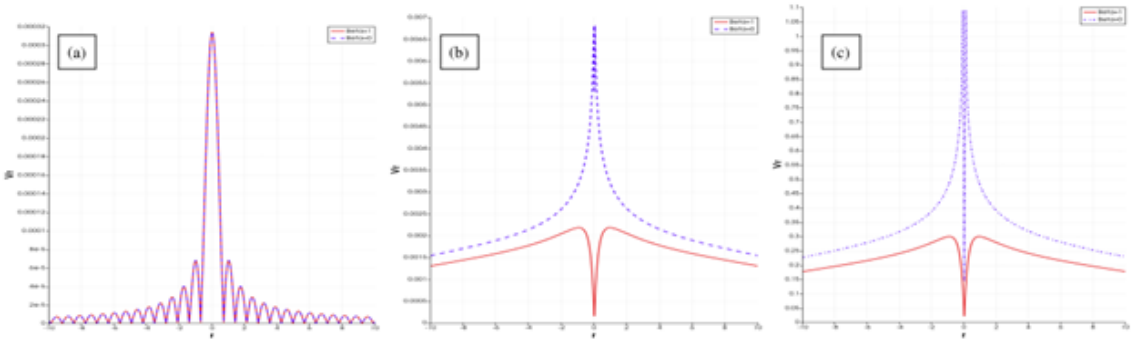

Figure 4: The comparison of radial velocity $v_r = \sqrt{v_x^2 + v_y^2}$ at $\beta = 0$ and $\beta = 1$ for a) $t = 0$, b) $t = 1$, and c) $t = 1.7$ over line $y = x$.

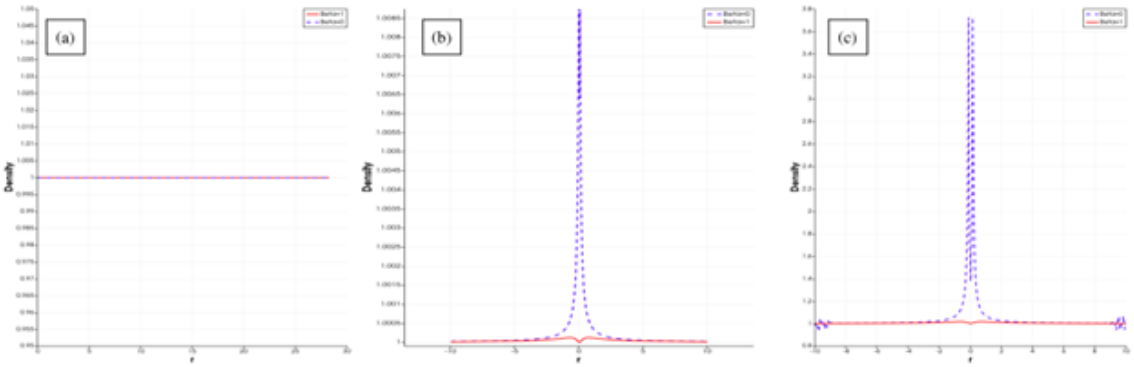

Figure 5: The comparison of plasma density at $\beta = 0$ and $\beta = 1$ for a) $t = 0$, b) $t = 1$, and c) $t = 1.7$ over line $y = x$.

Authors' Contributions

All authors have the same contribution.

Data Availability

No data available.

Conflicts of Interest

The authors declare that there is no conflict of interest.

Ethical Considerations

The authors have diligently addressed ethical concerns, such as informed consent, plagiarism, data fabrication, misconduct, falsification, double publication, redundancy, submission, and other related matters.

Funding

This research did not receive any grant from funding agencies in the public, commercial, or nonprofit sectors.

References

[1] Moreno-Insertis, F., Galsgaard, K., & Ugarte-Urra, I. 2008, ApJ, 673, L211.

[2] Shibata, K., & et al. 2007, Science, 318, 7.

[3] Cho, I. H., Moon, Y. J., Cho, K. S., & et al. 2019, ApJ, 884, L38.

[4] Cirtain, J. W., Golub, L., Lundquist, L., & et al. 2007, Science, 318, 1580.

[5] Craig, I. J. D., & Mc Clymont, A. N. 1991, ApJ, 371, L41.

[6] Craig, I. J., & Watson, P. G. 1992, ApJ, 393, 385.

[7] Longcope, D. W., & Priest, E. R. 2007, Phys. Plasmas, 14, 122905.

[8] McLaughlin, J. A., & Hood, A. W. 2004, A&A, 420, 1129.

[9] McLaughlin, J. A., Hood, A. W., & de Moortel, I. 2011, SSRv, 158, 205.

[10] Sabri, S., Vasheghani Farahani, S., Ebadi, H., Hosseinpour, M., & Fazel, Z. 2018, MNRAS, 479, 4991.

[11] Sabri, S., Vasheghani Farahani, S., Poedts, S., & Ebadi, H. 2020, Scientific Reports, 10, 15603.

[12] Goossens, M., An introduction to plasma astrophysics and magnetohydrodynamics, Volume 294 of Astrophysics and Space Science Library, October 2003.

[13] Van Doorsselaere, T., Srivastava, A. K., Antolin, P., Magyar, N., Vasheghani Farahani, S., & et al. Space Sci. Rev. 2020, 216, 140.

[14] Vasheghani Farahani, S., & Hejazi, S. M. 2017, ApJ, 844, 148.

[15] Vasheghani Farahani, S., Hejazi, S. M., & Boroomand, M. R. 2021, ApJ, 906, 70.

[16] Galsgaard, K., Priest, E. R, & Titov, V. S. 2003, J. Geophys. Res. Space Phys., 108, 1042.

[17] Thurgood, J. O. & McLaughlin, J. A. 2013, A&A, 555, A86.

[18] McLaughlin, J. A., & Hood, A. W. 2006, A&A, 452, 603.

[19] McLaughlin, J. A., De Moortel, I., Hood, A. W., & Bardy, C. S. 2009. A&A, 493, 227.

[20] Brown, D. S., & Priest, E. R. 2001, A&A., 367, 339.

[21] Gruszecki, M., Vasheghani Farahani, S., Nakariakov, V. M., & Arber, T. D. 2011, A&A, 531, A63.

[22] Bulanov, S. V., & Syrovatskii, S. I. 1980, Fiz, Plazmy, 6, 1205.

[23] McLaughlin, J. A., & Hood, A. W. 2005, A&A, 435, 313.

[24] Craig, I. J. D., & Fabling, R. B. 1996, ApJ, 462, 969.

[25] Pontin, D. I., & Glasgaard, K. 2007, J. Geophys. Res., 112, 3103.

[26] Nakariakov, V. M., Foullon, C., Verwichte, E., & Young, N. P. 2006, A&A, 452, 343.

[27] Mignone, A., Bodo, G., Massaglia, S., & et al. 2007, ApJS, 170, 228.

[28] Mignone, A., Zanni, C., Tzeferacos, P., & et al. 2012, ApJS, 198, 7.

[29] Karampelas, K., McLaughlin, J. A., Botha, G. J. J., & et al. 2022, ApJ, 925, 195.